REFERENCES

1. F. E. Carroll, American Journal of Roentgenology **179** 583 (2002)
2. E. Rubenstein, *et al.*, E Proc. Conf Digital Radiogr. 314, 42-49(1981).
3. S. Otsuka, *et al.*, British Journal of Radiology 72, 25-28(1999).
4. M. Uesaka, *et al.*, The XXI International LINAC Conference in Korea, 19-23 August (2002)
5. K. Dobashi *et al.*, submitted to Japan J. Appl. Phys.
6. GLC Project, KEK Report, 2003-7(2003).
7. A. Fukasawa, *et al.*, IJAEM **14** 221:
   Proceedings of The 2nd Asian Particle Accelerator Conference, 843(2001).

X-BAND LINAC BEAM-LINE FOR MEDICAL COMPTON SCATTERING X-RAY SOURCE

Katsuhiro Dobashi, National Institute of Radiological Sciences, Chiba, Japan
Mitsuru Uesaka, Atsushi Fukasawa, Futato Ebina, Tatsuo Kaneyasu,
Haruyuki Ogino, Fumito Sakamoto, Tomohiko Yamomoto, UTNS University of Tokyo, Ibaraki, Japan
Junji Urakawa, Toshiyasu Higo, Mitsuo Akemoto, Hitoshi Hayano, KEK, Tsukuba, Japan

Abstract

Compton scattering hard X-ray source for 10-40 keV are under construction using the X-band (11.424 GHz) electron linear accelerator and YAG laser at Nuclear Engineering Research laboratory, University of Tokyo. This work is a part of the national project on the development of advanced compact medical accelerators in Japan. National Institute for Radiological Science is the host institute and U. Tokyo and KEK are working for the X-ray source. Main advantage is to produce tunable monochromatic hard (10-40 keV) X-rays with the intensities of 10^8-10^9 photons/s (at several stages) and the table-top size. In addition, dual energy monochromatic X-ray source can be realized that generate two monochromatic hard X-ray by turin with high (up to 10 pps) repetition rate by one X-ray source.

The X-ray yield by the electron beam and Q-switch Nd:YAG laser of 2.5 J/10 ns is 10^7 photons/RF-pulse (10^8 photons/sec in 10 pps). X-band beam line for the demonstration is under commissioning. We also design to adopt a technique of laser circulation to increase the X-ray yield up to 10^8 photons/pulse (10^9 photons/s).

INTRODUCTION

Hard X-rays of 10-40 keV are now very useful in medical science, biology and material science. for exaple, Dynamic IVGAC[1, 2] and monochromaticd X-ray imaging, CT. In addition, Dual energy X-ray CT[3] and Substruction imaging with contrast agent and Dual energy X-ray are realized that require two monochromatic hard X-ray.

Intense hard X-rays are generated by a third generation light source. However, most SR sources are too large to be applied and used widely for public usage of the monochromatic hard X-ray. Therefore, we are developing a compact monochromatic hard X-ray (10-40 keV) source based on laser-electron collisions with the X-band (11.424 GHz) linac system[4]. One to ten percent narrow band X-rays are generated by collimating scattered photons that are related to the energy and scattering angle.

The final target of this study is an integrated system for medicine. as shown in Fig.1. This system is equipped with an X-band RF-source and a moving arm including an X-band linac, Q-switch laser system and X-ray detector.

A multi-bunch electron beam generated by a thermionic-cathode RF gun is collimated and compressed temporally by an alpha-magnet and accelerated by X-band accelerating structures. The electron beam is bent by the achromatic bends and focused at the collision point(CP). About a 10 ns hard X-ray is generated via Compton scattering upon laser-electron collision. After the collision, the electron beam is bent and decelerated by an X-band decelerating structure. The decelerated electron beam with an energy lower than 1 MeV is injected to a beam dump. In addition, this system can generate dual energy monochrmatic hard X-ray using two Nd:YAG laser by turn.

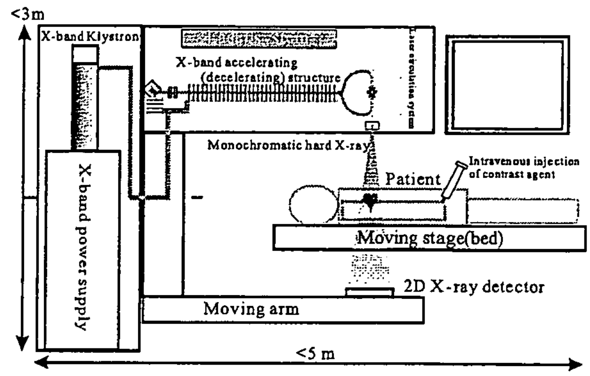

Figure 1: Final target of this study.

The laser system for collision is composed of a Q-switch Nd:YAG laser and a laser pulse circulating system to increase X-ray yield.

To demonstrate that the proposed X-ray source can be realized and will be useful in medicine, an X-band linac beam line for the proof-of-principle experiment shown in Fig. 2 is under construction. The X-ray yield by the electron beam and Q-switch Nd:YAG laser of 2.5 J/10 ns is 10^7 photons/RF-pulse (10^8 photons/sec in 10 pps). X-band beam line for the demonstration is under commissioning. We also design to adopt a technique of laser circulation to increase the X-ray yield up to 10^8 photons/pulse (10^9 photons/s).

In this paper, we present the design and numerical analysis of the X-ray source system to demonstrate hard X-ray generation and its applications.

X-BAND BEAMLINE FOR PROOF-OF-PRINCIPLE EXPERIMENT

Compact hard X-ray source based on the X-band linac that we propose is shown in Fig. 2. Multi-bunch beam generated by thermionic-cathode RF-gun is accelerated by X-band accelerating structures. The beam is bent and focused at the collision point. About 10 ns hard X-ray is generated via Compton scattering on laser-electron collision.

0-7803-8859-3/05/$20.00 ©2005 IEEE

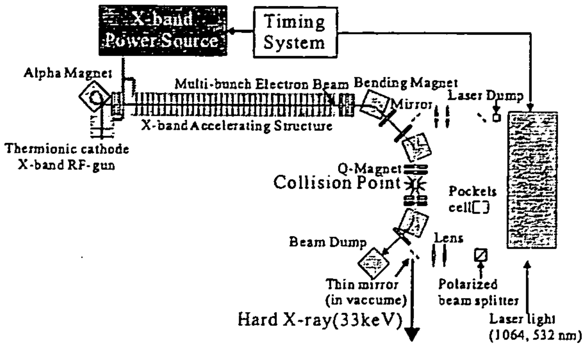

Figure 2: Schematic illustration of Compact Hard X-ray source based on thermionic-cathode X-band RF-gun, X-band accelerating structure and Q-switch Nd:YAG laser.

Beam energy	35 MeV
Charge/bunch	20 pC
bunches/RFpulse	10^4
Beam size(rms)(x,y)	100, 100 μm
Beam emittance(x,y)	10, 10 πmm·mrad

Table 1: Beam parameters at the collision point

X-band linac

X-band linac is applied to the compact hard X-ray source. RF-wavelength of the X-band is 1/4 of S-band (2.856 GHz). However, the maximum filed gradient as $\sim$ 40 MV/m enable remarkable compactness.

An X-band accelerating structure with 0.7 m long is used for the X-ray source. The technologies for X-band accelerating structure developed for future linear colliders[7] at KEK and SLAC are fully adapted for this development. At first, the RDS type accelerating structure has been adopted, which is already under manufacturing.

We adopt PPM type X-band Klystron (E3768A) designed for linear colliders[7]. Klystron Modulator is under design to fit this X-ray source. RF power is above 50MW in 1 μs.

The beam optics of the X-band linac beam line designed using SAD[8] code is shown in Fig.3. Beam parameters at the collision point (CP) are shown in Table 1.

Laser system

To concentrate on R&D of the accelerator, we choose a commercial and reliable laser for laser-electron collision.

To realize such a compact system, we adopt two Q-switch Nd:YAG laser with the intensity 2.5 J/pulse(1.4J/pulse for second harmonics), the repetition rate 10 pps, the pulse length 10 ns(FWHM) and wavelength of 1064 nm(fundamental).

In second step, to switch the X-ray energy immediately, we add the laser system. Each laser system for fundamental and second harmonics are shot by turn. Then we can generate dual energy monochromatic X-ray by turn with repetition rate of 12.5 Hz as shown in Fig.4. Advantage of the this dual energy X-ray source is the switing of X-ray energy with high repetition rate that is very useful for dynamic sustructon imaging and dual energy X-ray CT.

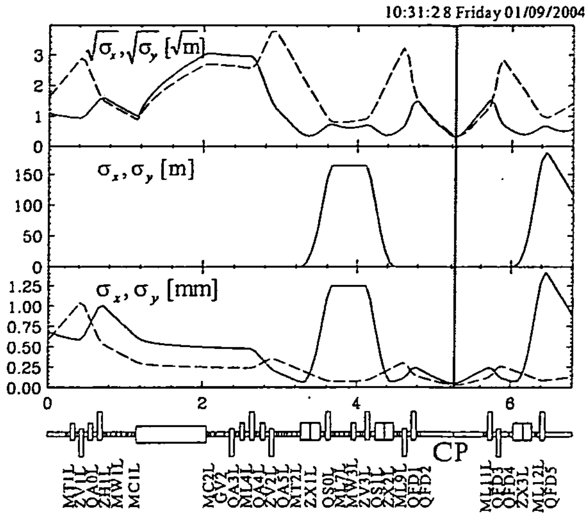

Figure 3: Beam optics for X-band linac.

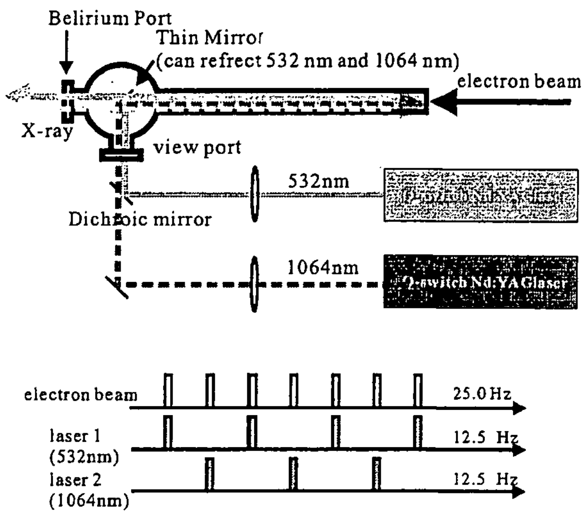

Figure 4: Concept of dual energy X-ray generation system.

To increase X-ray yield, we have to design the technique of circulation of laser pulse, which enhance the luminosity by 10 times. Detail of the laser pulse circulation system will be report in another paper.

X-ray yield and properties

The X-ray yield per bunch is calculated with cross section of Compton scattering and Luminosity. Enegy distributions and energy due to scattering angle of the X-ray for each wavelength of laser light with electron beam energy 35MeV are shown in Fig.5. Property of the X-ray is summalized in Table 2

Figure 6 shows the mean energy and rms energy spread of the available X-ray for each laser wavelength when scat-

 0-7803-8859-3/05/$20.00 ©2005 IEEE

laser wavelength (nm)	1064	532
pulse energy of laser (J/pulse)	2.5	1.4
Xray yield (photons/pulse)	9.9×10^6	4.4×10^6
Maximum X-ray energy(keV)	21.9	43.8

Table 2: Properties of the generated X-ray with electron beam energy 35 MeV, charge 20 pC/bunch

tered photon are collimated with each collimated angle.

TEST OF X-BAND RF SOURCE AND X-BAND THERMIONIC CATHODE RF-GUN

Test of RF generation and RF aging of the X-band klystron is under way. Peak power of RF is estimated to 10 MW per RF output port of the klystron. Total output power is 20 MW and pulse length 600 ns, repetition rate 5 pps.

After RF parameters ware reached to required by the RF-gun experiment, we started RF-aging of the X-band thermionic cathode RF-gun. Detail of the exprtiment will be shown in another presentaion.

Next of the RF-gun experiment, Klystron aging is continuled to reach the RF parameter upto 50 MW, 1 μs, 5 pps. Then, X-band acceleratinc structure is installed and acceleration test and X-ray generation will be performed at this autumn.

APPLICATION

Many application of monochromatic hard X-ray is proposed and performed with 3rd generation SR source. Main purpose of this study is demonstration of these applicaton in proposed X-ray source.

After the X-ray generation experiment, we start the experiment for application, for example, Dual energy X-ray CT. Detail of the applicaton experiment is reported in another presentation.

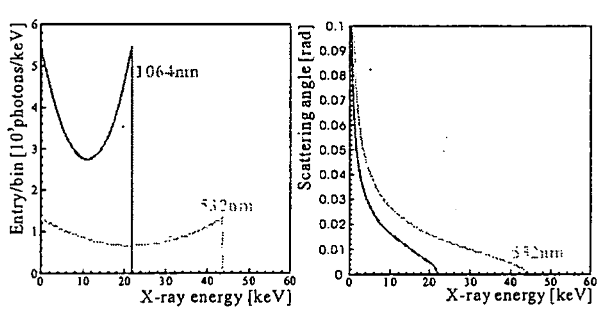

Figure 5: Energy spectrum of X-ray for laser wavelength of 1064 and 532 nm with electron beam energy 35 MeV.

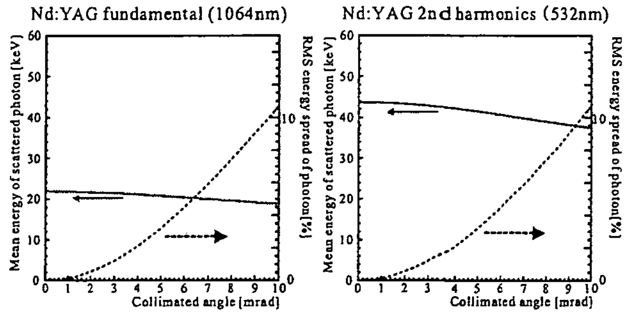

Figure 6: Energy spred in rms and mean energy of available X-ray with each collimated angle.

CONCLUSION

We are developing the compact X-ray source by laser-electron collision based on the X-band linac for medicine. To realize a remarkably compact system, we adopt the X-band system and commercial Q-switch laser. The X-ray yield by the electron beam and Q-switch Nd:YAG laser of 2.5 J/10 ns is 10^7 photons/RF-pulse (10^8 photons/sec in 10 pps). We also design to adopt a technique of laser circulation to increase the X-ray yield up to 10^8 photons/pulse (10^9 photons/s).

Final target of this study is the integrated system for medicine shown in Fig. 5. This system has X-band RF-source and moving arm including X-band linac, Q-switch laser system and X-ray detector. We can perform dynamic IVCAG so as to CAG and can get clear dynamic image of coronary artery with less distress for patients.

ACKNOWLEDGEMENTS

This study is performed in the national project of "Development of Advanced Compact Accelerators" in Japan, partially supported by Research Program on Development of Innovative Technology (#0494) in Japan Science and Technology Agency.

REFERENCES

[1] E. Rubenstein, et al. *Proc. National Academy Sci. USA* 83(1986)24, p.9724.

[2] S. Ohtsuka, et al. *British Journal of Radiology* 72(1999) p.24.

[3] M Torikoshi, et al. *Opt.* 6 371(2000).

[4] K. Dobashi, et al. *Jpn. J. Appi. Phys.* 444A pp.1999-2005(2005).

[5] K. Dobashi, et al. *Proc. 8th European Particle Accelerator Conference in Paris*, France, 667(2002).

[6] M. Uesaka, et al. *Proc. XXI International LINAC Conference in Korea*, August 19 - 23, Gyeongju, Korea, 626(2002).

[7] GLC report *KEK report* 2003-7(2003).

[8] K.Hirata; An introduction to SAD(Strategic Accelerator Design), Second Advanced ICFA Beam Dynamics Workshop, CERN 88-04 (1988)

Proceedings of 2005 Particle Accelerator Conference, Knoxville, Tennessee

DUAL-ENERGY X-RAY CT BY COMPTON SCATTERING HARD X-RAY SOURCE

Tatsuo Kaneyasu, Mitsuru Uesaka*, Nuclear Professional School, University of Tokyo, Japan
Katsuhiro Dobashi, Masami Torikoshi, National Institute of Radiological Sciences, Chiba, Japan

Abstract

We are developing a compact Compton scattering hard X-ray source by the X-band linac and YAG lasers at Nuclear Professional School, University of Tokyo. The compact hard X-ray source can produce tunable monochromatic hard X-rays for 10 - 40 keV. The monochromatic hard X-rays are very useful in large fields of medical and biological sciences. We are planning to carry out dual-energy X-ray CT, which enables us to obtain 3D distribution of effective atomic number Z_{eff} and electron density ρ_e in a matter. The hard X-ray source has an advantage in the dual-energy X-ray CT. The X-ray energy can be changed quickly by introducing a fundamental-frequency and a second-harmonic-frequency lasers. It is indispensable to change the X-ray energy quickly for medical imaging, but it is very difficult to achieve the quickness with a large SR light source and others. The information on the atomic number and electron density will be used for radiation treatment planning as well as for identification of materials in a nondestructive test. We examined applicability of the dual-energy X-ray CT for low to medium Z elements ($Z \leq 38$) by considering the X-ray energy profile generated by the Compton scattering hard X-ray source.

INTRODUCTION

Monochromatic hard X-rays are required in large fields of medical and biological applications. Intense hard X-ray is generated by SR light sources, but most of SR light sources are too large for widely applications. Therefore, a compact hard X-ray source is needed for wide use of monochromatic hard X-ray. We have developed a compact Compton scattering hard X-ray source [1, 2] using an X-band linac as presented in Fig. 1. The compact hard X-ray source can produce tunable monochromatic (1 to 10 % energy spread rms) hard X-rays for 10 - 40 keV. We are planning to perform dual-energy X-ray CT using monochromatic hard X-ray, which enables us to obtain cross sectional image of a material based on effective atomic number Z_{eff} and electron density ρ_e. Experiments for the dual-energy X-ray CT has been carried out utilizing SR light sources to measure electron density in biological materials [3, 4]. The electron density in a biological material was measured in agreement within 1 % of the theoretical one [3]. We will use the dual-energy X-ray CT for atomic number analysis in a material. For instance, the information on atomic number distribution in a tumor will contribute to treatment planning for advanced radiotherapy. Atomic number images in a plant are needed in plant physiology. In a nondestructive test of radioactive waste, we need to identify elements of a material. So far, the dual-energy X-ray CT has been performed for biological materials which consist of light elements of $Z \leq 20$. To apply the dual-energy X-ray CT for wide-range atomic numbers, we have carried out a numerical simulation and examined the applicability of the method by considering the X-ray profile of the compact hard X-ray source. Furthermore, we are planning to apply the compact hard X-ray source for micro vessel angiography and protein structural analysis.

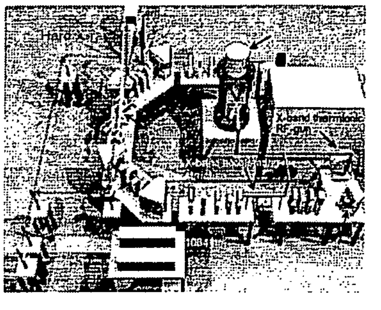

Figure 1: Schematic drawing of the compact hard X-ray source based on Compton scattering.

DUAL-ENERGY X-RAY CT

Theoretical Background

Effective atomic number Z_{eff} and electron density ρ_e are obtained by linear attenuation coefficients of a material using two monochromatic X-rays with different energies. A linear attenuation coefficient μ of a material is approximately written as a function of atomic number Z and X-ray energy E using a formula proposed by Jackson and Hawkes [6], as follows;

$$\begin{aligned}\mu(Z,E) \simeq & \rho\frac{N_A}{A}Z\{4\sqrt{2}Z^4\alpha^4(\frac{mc^2}{E})\phi_0\sum_{nll'}f_{nll'} \\ & + \sigma_{\text{KN}} + \frac{Z(1-Z^{b-1})}{Z'^2}\sigma_{\text{SC}}^{\text{coh}}(Z',E')\} \\ = & \rho_e(Z^4F(Z,E)+G(Z,E))\end{aligned} \quad (1)$$

where, ρ is mass density, N_A is Avogadro's number, A is atomic mass, $f_{nll'}$ is the collection terms for photoelectric absorption cross section, σ_{KN} is the Klein-Nishina cross section and $\sigma_{\text{SC}}^{\text{coh}}$ is the coherent scattering cross section of the standard element Z' at energy of $E' = (Z'/Z)^{1/3}E$.

* uesaka@utnl.jp

0-7803-8859-3/05/$20.00

In the equation, parameter b is proposed to be 0.5 and the standard element is Oxygen [6]. When linear attenuation coefficients are measured for two energies E_1 and E_2, one can extract effective atomic number Z_{eff} and electron density ρ_e by solving following equations;

$$Z^4 = \frac{\mu(E_2)G(Z,E_1) - \mu(E_1)G(Z,E_2)}{\mu(E_1)F(Z,E_2) - \mu(E_2)F(Z,E_1)}, \quad (2)$$

$$\rho_e = \frac{\mu(E_1)F(Z,E_2) - \mu(E_2)F(Z,E_1)}{F(Z,E_2)G(Z,E_1) - F(Z,E_1)G(Z,E_2)}. \quad (3)$$

The effective atomic number Z_{eff} is defined for a compound or a mixture as;

$$Z_{\text{eff}} = \left(\sum_i q_i Z_i^k\right)^{1/k} \quad (4)$$

where q_i is the fractional electron content of ith element in the compound or the mixture and the parameter $k = 4$.

This dual-energy method is limited by the K-edge energy of a material because the equation (1) can not be applied below K-edge energy. We will operate the compact hard X-ray source as electron beam energy is 35 MeV and the wavelength of the laser is 1064 nm and 532 nm. In this situation, the maximum X-ray energies are 21.9 keV and 43.8 keV. The X-ray energy should allow us to identify elements up to $Z = 38$. Energy spread $\Delta E/E$ of the monochromatic hard X-ray generated by SR is in the order of 10^{-4}, but the energy spread in the compact hard X-ray source is expected to be 1 to 10 % (rms), which is dependent on the collimator angle [2]. The energy spread of the X-ray is negligible with SR light sources, but in the case of the Compton scattering X-ray source the energy spread affects the accuracy of atomic number identification.

To examine the applicability of the dual-energy X-ray CT with the compact hard X-ray source, we have performed a numerical simulation for low to medium Z elements ($Z \leq 38$). We adopt linear attenuation coefficients of materials listed in the photon cross section database [7] in the simulation. The geometry of the dual-energy X-ray CT system in the simulation is shown in Fig. 2. We assumed a point light source and the thickness and width of the sample is 1 mm and 20 mm, respectively. In this case, X-ray photons are collimated at 3.3 mrad. It is noted that the X-ray energy of the Compton scattering X-ray source is dependent on the scattering angle. Thus, the X-ray energy is unique on each pixel of the 2D detector. When pixel size is 0.5 mm, $\Delta\theta$ is less than 0.2 mrad and the energy spread in the pixel is in the order of 0.1 %. This small energy spread in the pixel should improve accuracy of the dual-energy analysis. Effective atomic numbers obtained by the linear attenuation coefficients for two energies on each pixel of the detector are shown in Fig. 3(a). Average of the Z_{eff} is plotted as a function of atomic number of sample Z_{samp} in Fig. 3(b). The accuracy of estimated effective atomic number $\Delta Z/Z$ is less than 3 % (rms) except for $Z = 25$ and 33. We confirmed that atomic number can be identified up to $Z = 38$ using 21.9 keV and 43.8 keV X-rays with enough accuracy even energy spread of the monochromatic X-ray is 1 to 10 %. The limitation of this method is due to K-edge energy of the material.

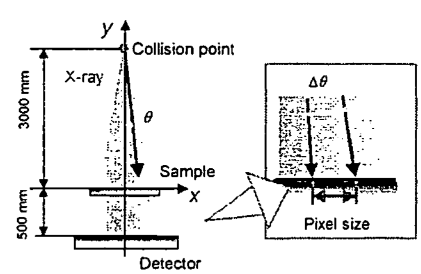

Figure 2: Schematic drawing of the dual-energy X-ray CT system using the compact monochromatic hard X-ray source.

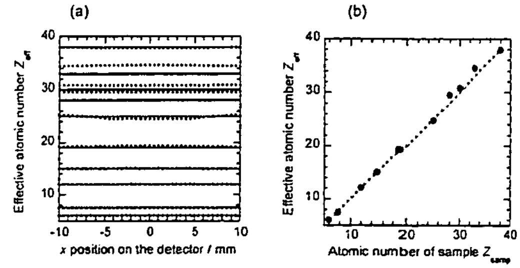

Figure 3: (a) Effective atomic number Z_{eff} on each pixel of the detector. The solid circles indicate identified effective atomic number Z_{eff}. (b) Average of the effective atomic numbers.

CT Simulation

A numerical CT simulation has been carried out with low to medium Z elements. We assumed CT system as already shown in Fig. 2 with cylindrical samples. The diameter of the sample is 20 mm and the pixel size of the detector is 0.1 mm. First, light elements of $Z = 13, 15$ and 19 with water as presented in Fig. 4(a) is tested. Reconstructed cross sectional images of the sample based on linear attenuation coefficients are obtained for two energies. Solving the equations (2) and (3), atomic number in the image is derived from linear attenuation coefficients based images. Two-dimensional images based on effective atomic number distribution in the sample and the reconstructed image are shown in Fig. 4. Atomic number distributions of both images at $y = 0$ are compared in Fig. 5(a). As shown in Fig. 5(a), atomic number in the material is well analyzed for light elements of $Z = 13, 15$ and 19 with $\Delta Z/Z_{\text{samp}}$ is 2.1, 5.0 and 7.2 % (rms), respectively. The poor accuracy for the element of Z=19 is caused by the reconstruction method and it will be improved.

This analysis can be applied to medium Z elements up to $Z = 38$. We have simulated CT image by assuming a sample consists of medium Z elements shown in Fig. 6(a). As shown in Fig. 6(b), the medium Z element of $Z = 38$ is also identified with $\Delta Z/Z_{samp}$ is 2.7 % (rms). The atomic number distribution of the reconstructed image at $y = 0$ is compared with that of the sample in Fig. 5(b). We have found that the dual-energy X-ray CT can be used to identify medium Z elements ($Z \leq 38$) in a material using the Compton scattering X-ray source with X-ray energies of 21.9 keV and 43.8 keV.

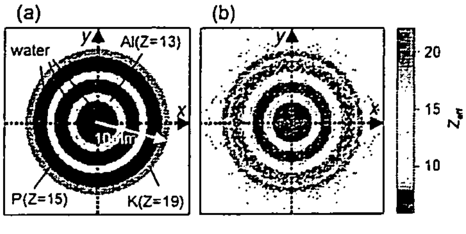

Figure 4: (a) Atomic number distribution in the sample. (b) Atomic number distribution in the reconstructed image.

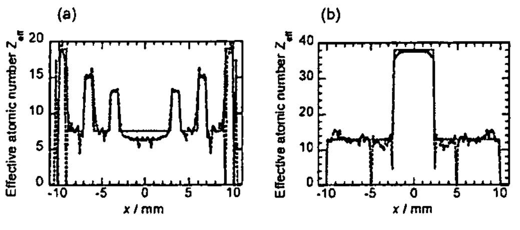

Figure 5: Atomic number distributions at $y = 0$ for sample and reconstructed images in (a) Fig. 4 and (b) Fig. 6. The dotted line indicates effective atomic number Z_{eff} and the solid line indicates atomic number of the sample.

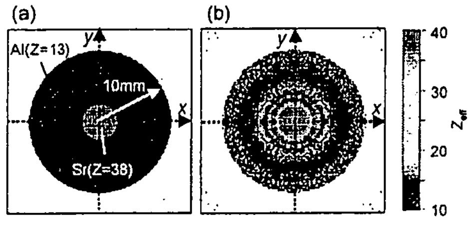

Figure 6: (a) Atomic number distribution in the sample. (b) Atomic number distribution in the reconstructed image.

APPLICATIONS

As already mentioned above, the dual-energy X-ray CT should be a powerful tool for identification of elements in a material. Atomic number distribution measurement will contribute to treatment planning in advanced radiotherapy. We will reveal the availability of atomic number distribution in a tumor using the Monte-Carlo code "EGS4" for a treatment planning. In the biological application, a combination of the dual-energy X-ray CT and the neutron radiography is planned. Neutron radiography enables us to obtain water images in a living plant [5]. The combination of the dual-energy X-ray CT and the neutron radiography is useful to study movement of specific elements in a living plant. The hard X-ray source has an advantage for the dual-energy X-ray CT. The X-ray energy can be changed quickly by introducing a fundamental-frequency and a second-harmonic-frequency lasers. The switching time of the two lasers is planned to be 40 ms. It is needed to change the X-ray energy quickly for the dual-energy X-ray CT in medical and biological applications. Furthermore, the compact hard X-ray source will be applied to micro vessel angiography and protein structural analysis. The micro vessel, diameter of 25 μm, is already observed by SR light. Recently, micro vessel angiography has been performed using X-ray tube combined with the HARP camera in a small laboratory. The micro vessel angiography system will be constructed utilizing the compact X-ray source combined with the HARP camera.

SUMMARY

We have examined the applicability of the dual-energy X-ray CT using the compact hard X-ray source by a numerical simulation. Low to medium Z elements up to Z=38 are well identified with X-ray energies of 21.9 keV and 43.8 keV. Though the energy spread of monochromatic X-ray is 1 to 10 %, the X-ray energy profile depends on the scattering angle. Therefore, the energy spread of X-ray in a pixel is in the order of 0.1 %. The small energy spread in a pixel is an advantage of the Compton scattering X-ray source for the dual-energy X-ray CT. In addition, the X-ray energy can be changed quickly by introducing the two lasers. The quickness is very important advantage of the X-ray source for the dual-energy X-ray CT in medical and biological applications.

ACKNOWLEDGEMENT

The work on development of the X-ray source is performed in the national project of gDevelopment of Advanced Compact Acceleratorsh in Japan and partially supported from Research Program on Development of Innovative Technology in Japan Science and Technology Agency. The study on applications of the X-ray source is supported by the Japanese Ministry of Education, Culture, Sports, Sciences, and Technology and the Japanese Ministry of Health, Labor and Welfare.

REFERENCES

[1] K. Dobashi *et al.*, Proc. 8th European Particle Accelerator Conf. in Paris, France, 2002, p.67.

[2] K. Dobashi *et al.*, Jpn. J. App. Phys. **44** 1999 (2005).

[3] M. Torikoshi *et al.*, Phys. Med. Biol. **48**, 673 (2003).

[4] T. Tsunoo *et al.*, IEEE Trans. NS **50**, 1678 (2003).

[5] T. M. Nakanishi *et al.* J. Radioanal. Nucl. Chem. **255** 149 (2003).

[6] Daphne F. Jackson and D. J. Hawkes, Phys. Rep. **70** 169 (1981).

[7] XCOM http://physics.nist/gov/XCOM

X-BAND THERMIONIC CATHODE RF GUN AT UTNL

A. Fukasawa, T. Kaneyasu, F. Sakamoto, F. Ebina,
H. Ogino, M. Uesaka, UTNL, Naka, Ibaraki 319-1188 Japan
K. Dobashi, NIRS, Chiba, Chiba Japan 263-8555 Japan
J. Urakawa, T. Higo, M. Akemoto, H. Hayano, KEK, Tsukuba, Ibaraki 305-0801 Japan
H. Sakae, K. Matsuo, IHI, Yokahama, Kanagawa 235-8501 Japan

Abstract

A compact Compton scattering hard X-ray source is being developed at Nuclear Engineering Research School (old Nuclear Engineering Research Laboratory). This is considered to be used in the medical scene in the future. This system consists of 50 MeV X-band electron linac and YAG laser to produce 40 keV (fundamental) and 80 keV (the second harmonic). The linac has a thermionic cathode X-band RF gun and an alpha magnet as an injector. Traveling wave tube accelerate the beam up to 50 MeV.

The simulation shows the beam from the gun must be cut off its lower energy part. Alpha magnet with inner slits act as the role, and at the slit position 122 mm energy spread requirement was satisfied, but the charge became small. We must search better operation parameters.

A test beam line to demonstrate production of Compton scattering hard X-ray is under construction. Conditioning of a thermionic cathode X-band RF gun is being proceeded. Feeding with 1.5 MW 100ns was achieved (6 MW 400ns is required for test).

INTRODUCTION

Monochromatic hard X-rays enables advanced diagnostics such as dual X-ray CT[1] and IVCAG[2]. However the spectra of conventional hard X-ray sources are broad since they are bremsstrahlung radiation produced by electrons hitting against targets. A monochrometer can select narrow spectrum but the intensity decreases considerably. Only radiation at storage rings is possible to obtain sufficient intensity through a monochrometer. Its property is very good but the source has difficulty in its huge size for widely use. Compton scattering is one of the solutions to obtain narrow spectrum by putting a hole slit. Since it dose not require a monochrometer, the efficiency to obtain monochromatic X-ray becomes higher.

A compact Compton scattering hard X-ray source for medical use is developing at Nuclear Engineering Research Laboratory (UTNL) [3, 4]. It consists of 50 MeV electron linac and YAG lasers. In the first phase of this study, we will show the validity of our design by the production of Compton scattering hard X-ray. The test beam line is shown in Fig. 1 and the design parameters are in Table 1. The energy spread are required to be less than 1% for focusing at collision point. RF gun is introduced for its low emittance beam production. A thermionic cathode is expected pulse-to-pulse stable operation, although there are problems about backbomberedment. A thermionic carhode RF gun produces multibunch beam (in our case, 10^4 bunches in a 1μs-long RF pulse).

*fukasawa@utnl.jp

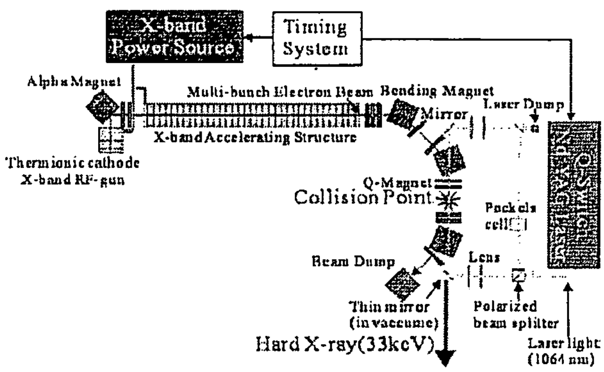

Figure 1: Beam line for a test of Compton scattering.

Table 1: Design parameters

Beam energy	35 MeV
Charge of a bunch	20 pC
Bunches in a pulse	10^4
Normalized emittance	10 πmm.mrad

THERMIONIC CATHODE RF GUN

The injector of this system consists of a thermionic cathode X-band RF gun and an α magnet. An α magnet is used to eliminate low energy particles by its inner slits. Bunch compression is also expected there. Since the energy spread after main acceleration is required to be less than 1%, beams from the injector must satisfy the following equation,

$$\delta = \frac{\Delta E_{inj} + E_{acc}\Delta\phi_{inj}^2}{E} < 0.01$$

where ΔE_{inj} is the energy spread at injector, $\Delta\phi_{inj}$ the bunch length in radians, and E_{acc} the energy gain in the main accelerating structure.

3.5-cell Cavity

Our gun cavity has 3.5 cells (Fig. 3) and is operated at π mode. Coaxial coupler [5] is introduced for axial symmetry of the field in the gun and to place inside solenoid coil. The cathode is dispenser type and the material is tungsten. It will be operated at the current density, 20 A/cm^2.

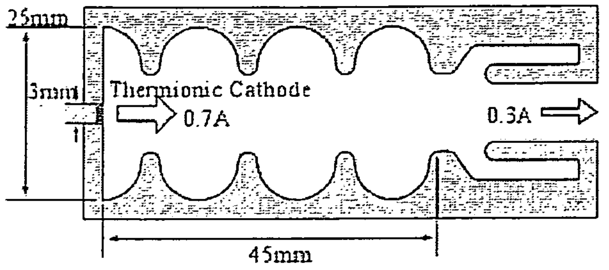

Figure 2: RF gun cavity.

Output of the Gun

The dynamics of the particles in the gun was simulated by PARMELA [6]. The total charge is 41 pC. The bunch length is 4.4 ps and the energy spread 0.16 MeV (those are rms over 2.25 MeV particles) (Fig. 3, 4). Since δ becomes 0.10, lower particles should be eliminated. When the particles less than 2.8 MeV is cut off, the bunch satisfy the energy spread condition (Fig. 5).

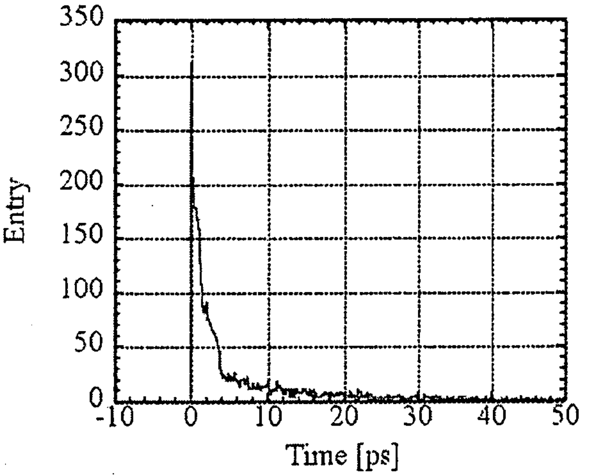

Figure 3: Bunch form (left) before alpha magnet.

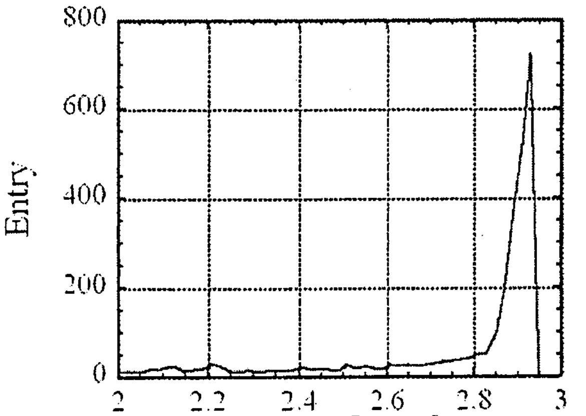

Figure 4: Energy spectrum (right) before alpha magnet.

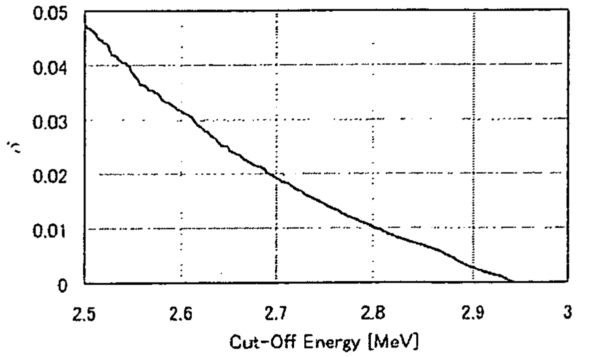

Figure 5: Relation between cut-off energy and estimated energy spread after main acceleration

Slit Position in α Magnet

The motion in the α magnet was calculated next. There is a slit to cut low energy particles in the α magnet. Moving this slit, the cut-off energy can be controlled (Fig.6). The bunch parameters after that are listed in Table 2. When the slit position is 121 mm, the condition is not satisfied. Although 122 mm satisfies it, the charge becomes small. Cut-off energy is higher than estimated in the previous section. This is because over bunching occur in α magnet and bunch length becomes longer. To obtain the best compression and high charge, the field gradient in the α magnet must be higher. However it is difficult to increase the field. Then the energy should be decreased.

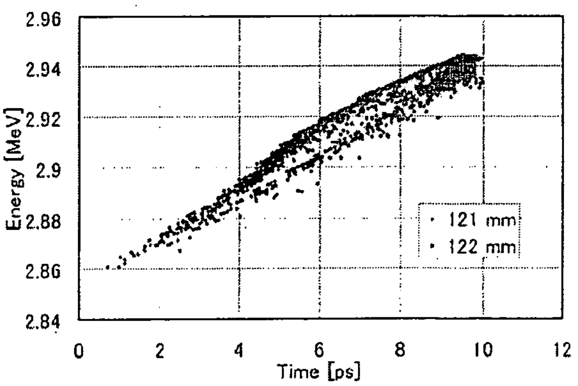

Figure 6: Particle distribution in time-energy space. Blue dots are for the slit position 121 mm and red for 122 mm.

Table 2: Bunch parameters after the α magnet

Position of slit	121 mm	122 mm
Charge	20.2 pC	7.5 pC
Energy	2.92±0.02 MeV	2.94±0.01 MeV
Cut-off energy	2.86 MeV	2.91 MeV
Normalized emittance	15.1, 6.3 πmm.mrad	10.2, 4.1 πmm.mrad
Bunch length	2.2 ps	1.0 ps
δ	0.024	0.005

PREPARATION FOR THE GUN TEST

The beam line for the test of the thermionic cathode X-band RF gun was constructed in this March. For the test the gun cavity must be processed by RF conditioning. After the conditioning beam experiment will be carried on.

Frequency Tuning

To check the tune of the cavity, we measured the return reflection from the gun. The pulse shapes of RF propagating forward and backward are shown in Fig. 7. The pulse propagating forward has spike in the head. Since there are no circulators which could sustain high power at X-band frequency, the reflected pulse returns back into klystron directly and come back to the gun again affecting the forward pulse.

To find a lowest reflection, frequency survey is performed. The minimum of the return loss are observed at 11.42450 GHz (Fig. 8). We changed the operation frequency 11.42400 to 11.42450 GHz.

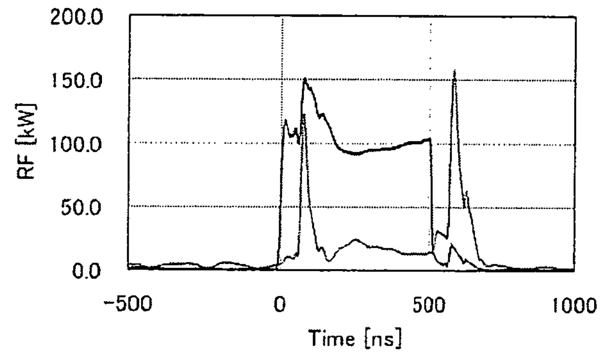

Figure 7: RF pulse shape into (blue) and reflected back from the gun cavity.

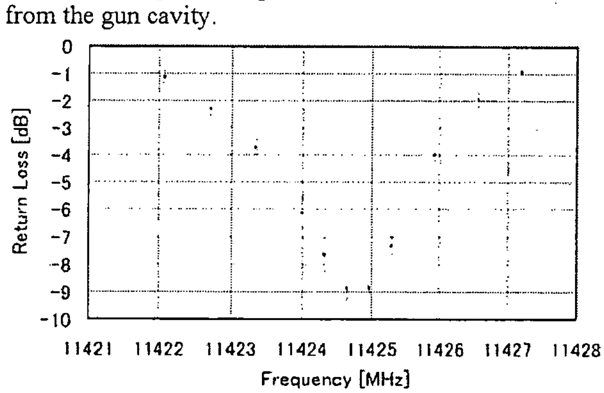

Figure 8: Return loss at the gun cavity.

RF Gun Conditioning

RF gun conditioning started in this April. The RF power 1.5 MW and the pulse length 100 ns achieved on May 13 while 6 MW and 400 ns is required for the test.

SUMMARY

We are developing a compact hard X-ray source. It requires the energy spread less than 1 %. Energy selection must be introduced and an alpha magnet with inner slits serves as that role. When the slit position came to 122mm, the condition was satisfied, however the charge became small. We are looking for better conditions.

A thermionic cathode X-band RF gun is being prepared for test. RF tuning was performed and 11.42450 GHz was chosen since the lowest reflection. RF gun conditioning began in this April. The RF status of the conditioning is now 1.5 MW 100ns while the goal is 6 MW 400ns.

ACKNOWLEDGEMENT

This study is a part of a national project, "Development of Advanced Compact Accelerators", and partially supported by Research Program on Development of Innovative Technology (#0494) in Japan Science and Technology Agency.

REFERENCES

[1] M. Torikoshi, et al., *Opt.* **6** (2000) 371.
[2] S. Ohtsuka, et al., *British Journal of Radiology* **72** (1999) 24.
[3] K. Dobashi, et al., *Jpn. J. Appi. Phys.* **444A** (2005) 1999.
[4] A. Fukasawa, et al., in the proceedings of APAC2001, Beijin, China (2001) 843.
[5] K. B. Kiewiet, et al., In the proceedings of EPAC2000, Vienna, Austria (2000) 1660.
[6] L. M. Young, Los Alamos National Laboratory report LA-UR-96-1834.

Available online at www.sciencedirect.com
SCIENCE DIRECT

NIMB
Beam Interactions with Materials & Atoms

ELSEVIER

Nuclear Instruments and Methods in Physics Research B 241 (2005) 905–908

www.elsevier.com/locate/nimb

Laser pulse circulation system for a compact monochromatic hard X-ray source

Futaro Ebina [a,*], Atsushi Fukasawa [a], Fumito Sakamoto [a], Haruyuki Ogino [a], Mitsuru Uesaka [a], Katsuhiro Dobashi [b]

[a] University of Tokyo, Nuclear Engineering Research Laboratory, 2-22 Shirakata-shirane, Tokai, Naka, Ibaraki 319-1188, Japan
[b] National Institute of Radiological Sciences, 4-9-1 Anagawa, Inage, Chiba, Chiba 263-8555, Japan

Available online 15 November 2005

Abstract

We developed a laser pulse circulation system for a compact source of monochromatic X-rays (10–60 keV) based on Compton scattering. In the X-ray source, laser pulses from a Q-switch Nd:YAG laser system collide with electron beams generated by a X-band linac. With the circulation system, a laser pulse collides with an electron beam multiple times, and the X-ray yield theoretically becomes 100 times larger than for one collision. In the proof-of-principle experiment, the laser intensity became larger by 10 times. Then, the X-ray yield will rise to at least 10^9 photons/s.

Keywords: X-band linac; Laser; X-ray source; Circulation

1. Introduction

1.1. Background

Monochromatic X-rays in the range of 10–60 keV are very useful for medical treatment, biology, material science and so on. For example, intravenous coronary arteriography (IVCAG) by monochromatic hard X-rays from synchrotron radiation (SR) has been proposed and tested in several institutes. Intense monochromatic hard X-rays (10^{11} photons/s for IVCAG) can be generated by third generation light sources. But most of SR light sources are large and expensive. Therefore, we aim to develop a compact monochromatic X-ray source (10–60 keV) based on Compton scattering shown in Fig. 1. We developed a laser pulse circulation system for the X-ray source. In the X-ray source with the circulation system, high power laser pulses repeatedly collide with multi-bunch electron beams, and the X-ray yield become larger.

* Corresponding author. Tel.: +81 29 287 8474; fax: +81 29 287 8471.
E-mail address: ebina@utnl.jp (F. Ebina).

0168-583X/$ - see front matter © 2005 Published by Elsevier B.V.
doi:10.1016/j.nimb.2005.07.237

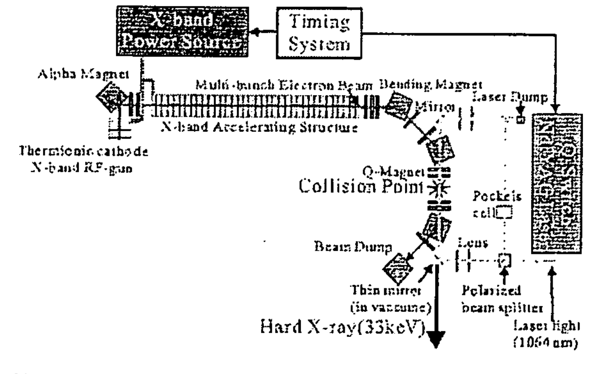

Fig. 1. Proposal for a compact monochromatic hard X-ray source.

1.2. X-ray yield

We consider the X-ray yield of our proposed system. Table 1 shows the properties of the electron and the laser beam. The X-ray yield per bunch is calculated by the known equation

$$N_{\text{X-ray}} = \sigma_{\text{comp}} L,$$

where σ_{comp} is the total cross section of Compton scattering and L is the luminosity of the laser pulse–electron bunch collision. Integrated luminosity per bunch L can be calculated by

$$L = (1 + \cos\varphi) \int_{-\infty}^{\infty} \int_{-\infty}^{\infty} \int_{-\infty}^{\infty} \int_{-\infty}^{\infty} \rho_l(x, y, s, t) \rho_e(x, y, s, t) \mathrm{d}x\, \mathrm{d}y\, \mathrm{d}s\, \mathrm{d}t,$$

where φ is the incident angle ($\varphi = 0$ for head-on collision), ρ_l and ρ_e are the spatial distribution function of the laser and the electron beams near the collision point, respectively. According to this equation, the system generates 10^7 photons/pulse (10^8 photons/s). The pulse length of the Q-switch Nd:YAG laser is 10 ns, and is shorter than the RF-pulse length (1 μs). This means that most of the electron bunches do not collide with the laser light. This is the reason why the laser pulse circulation system is effective to increase the X-ray yield.

Table 1
Properties of electron and laser beam of the X-ray source

Electron beam	
Kinetic energy	45 MeV
Charge	20 pC/bunch
Pulse width	1 μs
Number of bunches	10^4 bunches/pulse
Beam size	100 μm (rms)
Repeating ratio	10 pps
Laser pulse	
Wavelength	1064 nm
Pulse energy	2 J
Pulse width	10 ns (FWHM)

2. Laser pulse circulation system

Sketch of the laser pulse circulation system is shown in Fig. 2. Incident laser light passes through the polarizing beam-splitter and is focused at the collision point. After the laser pulse–electron beam interaction, the laser light is reflected by mirrors and its polarization plane is changed by the $\lambda/2$ waveplate and by the pockels cell. The polarization plane of the laser light is always vertical (s-polarization) at the polarizing beam-splitter and the laser pulse is reflected by the splitter. The laser light is led to the collision point again and can collide with the electron beam repeatedly.

3. Increase of X-ray yield

The total laser pulse energy in the laser circulation system I_N is

$$I_N = \sum_{n=0}^{N} I_0 A^n = I_0 \frac{1 - A^n}{1 - A},$$

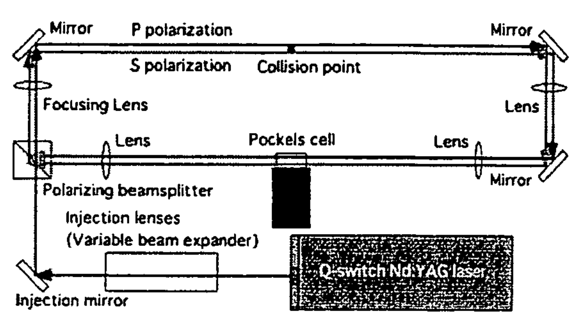

Fig. 2. Outline of the laser circulation system.

where I_0 is the initial pulse energy of the laser, A is the transmission efficiency per one circuit, and N is the total number of collisions. Since the revolving time is less than 25 ns, the laser light collides more than 40 times. With 90% transmission efficiency per collision ($A = 0.9$), we expect that the enhancement of X-ray yield becomes 10 times larger. Therefore, the X-ray source can generate 10^9 photons/s. As a next step of the laser pulse circulation, we will adopt a YAG rod as a gain medium in the circulation line to compensate the laser energy loss and achieve 100% transmission efficiency ($A = 1$). We will also utilize a higher energy laser pulse (more than 5 J) so that the X-ray yield will increase to 10^{10} photons/s.

4. Experiment

Before adding the laser pulse circulation system to the X-ray source, we are now doing a proof of experiment for the laser circulation system. The experimental setup is shown in Fig. 3. We use a relatively lower energy laser pulse (25 mJ) with ($\lambda = 532$ nm). The length of one circuit is 4 m and the revolving time is 13.3 ns.

For the laser–electron collision experiment, we have to control the laser profile and the electron beam profile at the collision point. The laser circulation system also requires high stability of the laser profile at the locus. Mirrors and lenses control the laser profile. The injection lenses (see Fig. 3) changes the beam size at the collision point, the beam size is inversely proportional to its beam size at the focusing lens. We move the angle of mirror B and the position of the focusing lens A to control the laser beam position at the collision point. We also move the mirror C and lens D to prevent an error due to the revolutions.

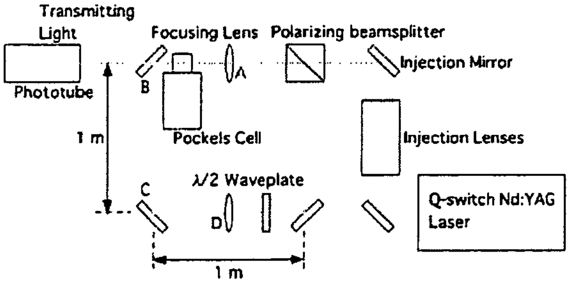

Fig. 3. Setup for the proof-of-principle experiment.

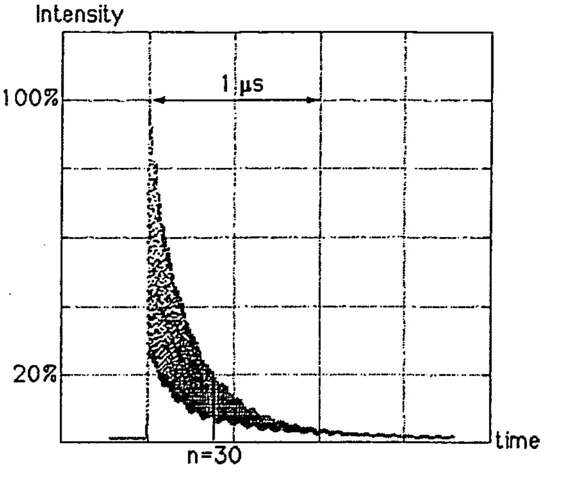

Fig. 4. Laser intensity in the circulation system.

5. Results

Fig. 4 shows the intensity of the laser pulse. This signal indicates that the laser pulse circulates more than 50 times (650 ns). The intensity of the 30th revolving pulse is approximately 20% of the incident laser pulse energy. The transmission efficiency is

$$I_0 A^{30} = 0.2 I_0,$$
$$I_0 = 94.7\%.$$

Therefore, the total X-ray yield will become more than 10 times larger, and the X-ray source will generate at least 10^9 photons/s.

6. Summary

We designed the laser pulse circulation system for the compact source of monochromatic hard X-rays. With 90% transmission efficiency, the X-ray yield becomes 10 times larger. We have been doing a proof of principle experiment and have proven that we can enhance the laser intensity by changing the laser's polarization plane. We will do further studies and experiments for the laser profiles control.

For further reading, see [1–6].

References

[1] M. Uesaka et al., Abstract of 21st Int. LINAC Conf. Korea, 2004, p. 174.

[2] K. Dobashi et al., Advanced Accelerator Concepts Workshop, America, in press.

[3] A. Fukasawa et al., presented at Asian Particle Accelerator Conf., China, 2001. Available from: <http://apac01.ihep.ac.cn/MA.html>.

[4] F. Ebina et al., Proc. First Particle Accelerator Meeting, Japan, 2004, p. 453.

[5] F.E. Carroll, Am. J. Roentgenol. 179 (2002) 583.

[6] A.E. Vieks et al., Abstract of 21st Int. LINAC Conf., Korea, 2004, p. 83.

Available online at www.sciencedirect.com

SCIENCE DIRECT

ELSEVIER

Nuclear Instruments and Methods in Physics Research B 241 (2005) 921–925

NIM B
Beam Interactions with Materials & Atoms

www.elsevier.com/locate/nimb

A tunable monochromatic hard X-ray CT composed of an X-band linear accelerator and a Q-switched laser

Atsushi Fukasawa [a,*], Mitsuru Uesaka [a], Fumito Sakamoto [a], Futaro Ebina [a], Katsuhiro Dobashi [b], Junji Urakawa [c], Mitsuo Akemoto [c], Toshiyasu Higo [c], Hitoshi Hayano [c]

[a] *Nuclear Engineering Research Laboratory, University of Tokyo, 2-22 Shirakata-Shirane, Tokai, Naka, Ibaraki 319-1188, Japan*

[b] *National Institute for Radiological Science, 4-9-1 Anagawa, Inage, Chiba 263-8555, Japan*

[c] *High Energy Accelerator Research Organization, 1-1 Oho, Tsukuba, Ibaraki 305-0801, Japan*

Available online 9 November 2005

Abstract

A Compton scattering hard X-ray source for 10–80 keV is under construction, which consists of an X-band (11.424 GHz) electron linear accelerator and a YAG laser. The main advantages are to produce tunable quasi-monochromatic hard X-rays (10–80 keV) with the intensities of 10^{8-10} photons/s (at several stages) and its tabletop size. The second important aspect is to decelerate the beams before the beam dumper to reduce the noise radiation there. This enables a 3rd generation synchrotron radiation source to be constructed in small facilities without heavy shielding. The final goal is to load this hard X-ray source on a moving gantry. This device will realize a tunable monochromatic X-ray CT and dual energy X-ray imaging, which determines 3D distribution of electron density and equivalent atomic number. This provides real physical information to diagnostics and curative program.

PACS: 29.27.−a

Keywords: Compton scattering; Hard X-ray; Linac; Deceleration

1. Introduction

A linac-and-laser-based Compton scattering system allows quasi-monochromatic hard X-rays to be obtained with a tabletop device. If the system is small and light enough, it is possible to be loaded on a gantry. We aim to use this monochromatic

* Corresponding author. Tel.: +81 29 287 8986; fax: +81 29 287 8488.

E-mail address: fukasawa@utnl.jp (A. Fukasawa).

0168-583X/$ - see front matter © 2005 Elsevier B.V. All rights reserved.
doi:10.1016/j.nimb.2005.07.210

hard X-ray source for medical applications. This system will provide clearer CT images with lower dose rate than a conventional one due to its monochromatic hard X-rays. Using two different energy X-rays, we can obtain a picture of the electron density and the effective atomic number distribution in 3D [1]. Drug delivery system is also one of the applications to be considered for our X-ray source. Putting X-ray sensitizers in nano-micells instead of drugs, the diseased part can be seen clearly or treated efficiently by using monochromatic X-ray at the required energy.

2. Development at UTNL

In our laboratory, Nuclear Engineering Research Laboratory, University of Tokyo (UTNL), a Compton scattering hard X-ray source is under construction and will start to operate in this winter. In Table 1 the design parameters of our system are listed. This system is designed at first to produce 33 keV hard X-rays for angiography [2,3] (Phase I). Tuning the accelerating phase and selecting the laser wavelength, this system will be able to produce X-rays in the range 10–80 keV (Phase II).

3. Compact hard X-ray source based on a 'soft dumping' linac

In Phase I and II system however, after the production of hard X-rays, the electron beams are dumped at high energy and produce strong radiation, which requires heavy radiation shielding, thus requiring the source to be fixed. Therefore, we propose a 'soft dumping' linac in which electron beams are decelerated to lower energy before dumped. Lower energy electrons produce much lower radiation (radiation is approximately proportional to γ^3, γ is Lorenz factor), and result in much smaller amount of shielding.

In this design we change the target X-ray energy to 40 keV, which is required for the application to dual X-ray imaging. These X-rays are produced by the collision of 47.4 MeV electrons with a 1064 nm laser which is the fundamental wavelength of Nd:YAG laser. By selecting the second harmonic generation, we can easily obtain 80 keV X-ray.

This linac is made of an X-band accelerator, which is smaller than conventional S-band one. A thermionic cathode RF gun is introduced. The main accelerator consists of four standing wave structures. Two structures are designed to have the same properties, combined through 3 dB hybrid and placed not to return the reflected RF from the cavity to the RF source.

To decelerate electron beams, we adopt counter-propagating deceleration. Both accelerating and decelerating beams travel in the same structure to the opposite direction. After the interaction point, beams are re-injected into the exit of the accelerating structure. Since the beams go to the opposite directions, standing wave structures are required to achieve both the acceleration and the deceleration.

4. Beam optics

The design of the lattice after acceleration is one of the important problems, since the transportation system could occupy larger space than the accelerating section. Also the magnets should be as few as possible. Our current lattice design is

Table 1
Design parameters of the hard X-ray source at NERL

	Phase I	Phase II
Electron beam energy	43 MeV	47 MeV
Charge	200 nC/pulse (= 20 pC × 10^4 bunches)	
Laser wavelength	1064 nm	532, 1064 nm
Laser power	2 J/pulse	5 J/pulse
X-ray energy	33 keV	10–80 keV
X-ray yield	1.7×10^9 photons/s	10^{10} photons/s

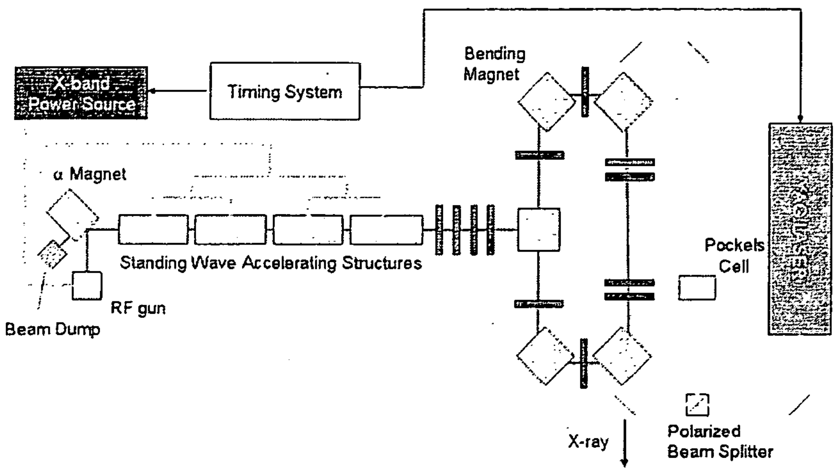

Fig. 1. Compact hard X-ray source based on a 'soft dumping' linac.

shown in Fig. 1. From the exit of the accelerating section, the beam goes through the matching section of three quadrupole magnets. All the bending magnets are the same: the bending angle is 90° and the bending radius 200 mm. The beams travel achromatically and isochronously in the bending system, and are focused at the interaction point by final doublet. Then beams go back to deceleration section through the lattice symmetrical at the interaction point.

A restriction of achromatic transportation requires $R_{16} = R_{26} = 0$ there. At the same time, the longitudinal bunch form should be the same as those right after the acceleration to decelerate the beams effectively. This requires $R_{56} = 0$ at the re-injection to decelerate the beam. We will design

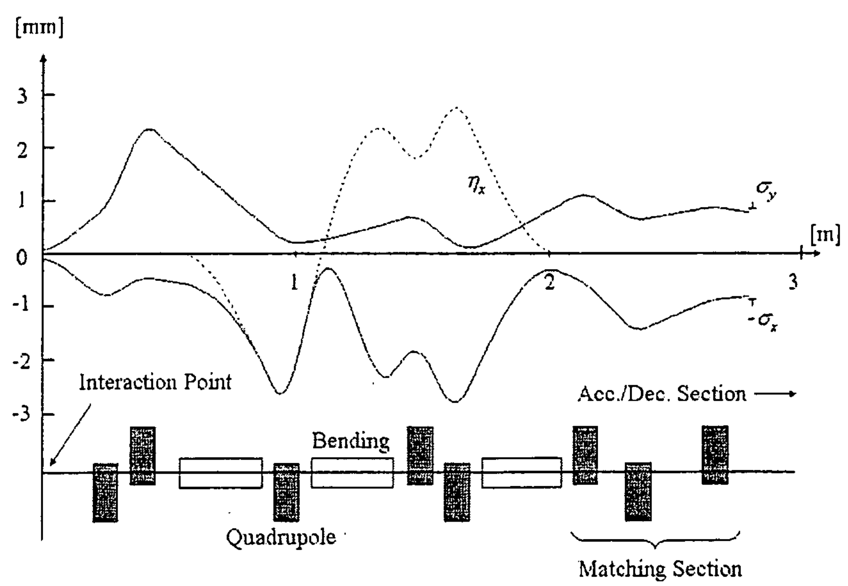

Fig. 2. Beam envelope in the arc part.

the lattice to be symmetrical at the interaction point, then $R_{56} = 0$ also required there.

PSI GRAPHIC TRANSPORT [4] (based on TRANSPORT [5]) is used to calculate the beam optics. Fig. 2 shows the beam envelope from the interaction point to the exit of the accelerating structure. The dispersion function becomes 0 after the transportation, and beams are focused into about 100 μm (rms). $R_{56} = 0$ is achieved at the exit of the accelerating structure.

In this design, the width of the transportation arc is about 1.5 m. This is still wide for a movable device, such as a hard X-ray gantry. We will proceed to minimize the lattice.

5. Beam tracking

PARMELA is used to calculate the beam motion. We used the result of the beam parameters after the alpha magnet (Table 2) to evaluate the optics and the deceleration of the beam. The rms spot size of the beam is $76 \times 61\ \mu m^2$. This is near the designed value. This shows success in the achromatic transportation. The longitudinal bunch forms after the transportation is shown in Fig. 3. The bunch length could not be maintained after the transportation, but the main part of the bunch stays in the deceleration phase. With the RF phase tuned to decelerate the main part, the average energy becomes 4.6 MeV (Fig. 4). Taking into account on the energy dependence of radiation, γ^3, $\sqrt[3]{\langle\gamma^3\rangle}$ is about 4.9 MeV. This means the radiation power produced by this beam is equivalent to that by 4.9 MeV beam.

Table 2
Parameters of the bunch after the alpha magnet

Charge	20 pC
Energy	3.5 MeV
Emittance	10π mm mrad

The achromatic system works well while the isochronous system is not successful. In the isochronous system, the error in the longitudinal position is originated from the large bending angle. To reduce this effect we should redesign the lattice with weaker bending magnets.

6. Summary

A Compton scattering hard X-ray source for medical applications is under construction at UTNL and the experiment of the beam acceleration is planned in 2005. We also proposed a linac, which has a decelerating section before the beam

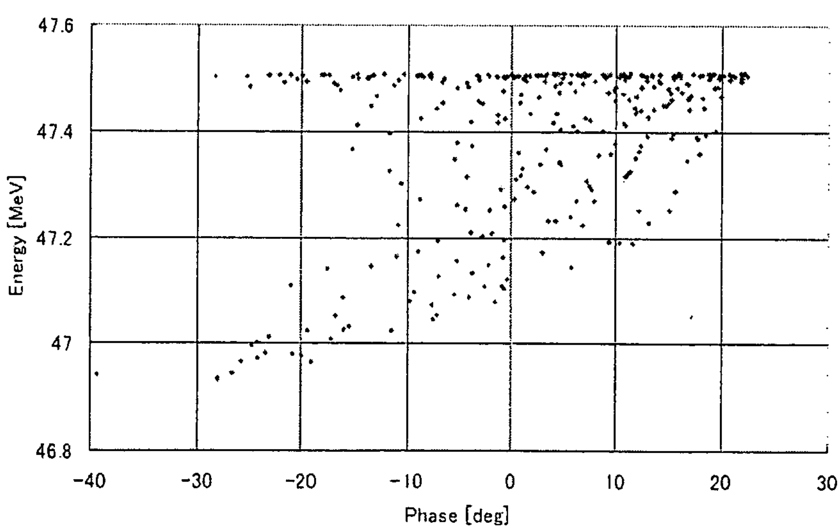

Fig. 3. Energy distribution before the deceleration.

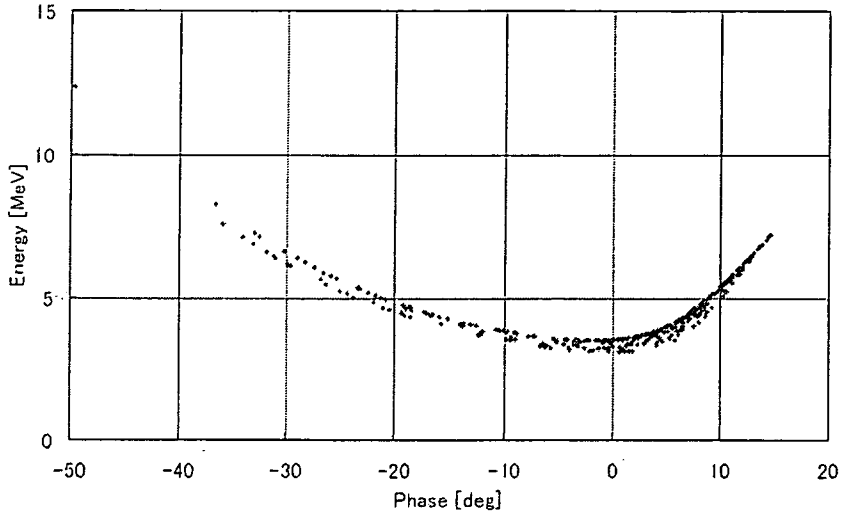

Fig. 4. Energy distribution after the deceleration.

dumper to reduce the noise radiation there. In our first design of the linac, the beam transportation is successful to make an achromatic system. We have shown the deceleration in the same structure as the acceleration, although isochronous system is not sufficient to decelerate the beam effectively.

Acknowledgements

This research is a part of a project, "Development of Advanced Compact Accelerator", funded by Ministry of Education, Culture, Sports, Science and Technology of Japan. We appreciate the staffs' dedicated support.

References

[1] M. Torikoshi et al., J. Biomed. Opt. 6 (2001) 371.
[2] A. Fukasawa et al., in: Proceedings of APAC 2001, (2001) 843.
[3] M. Uesaka et al., in: Proceedings of Linac 2002, (2002) 626.
[4] PSI Graphic Transport Framework by U. Rohrer based on a CERN-SLAC-FERMILAB version by K.L. Brown et al. Available from: <http://pc532.psi.ch/trans.htm>.
[5] K.L. Brown et al., See yellow reports CERN 73-16 (1973) and CERN 80-04 (1980).

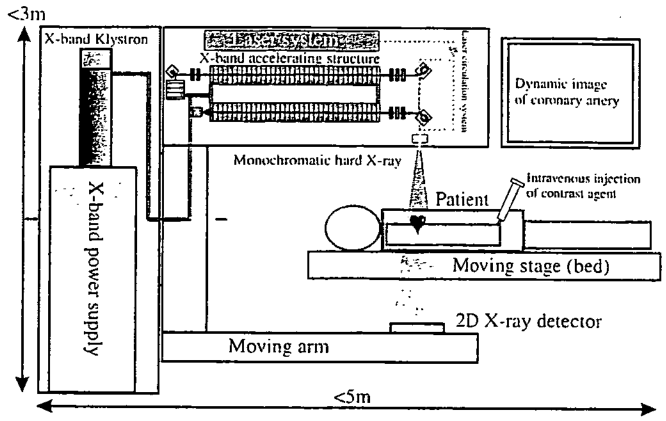

Fig. 2. Final target of this study.

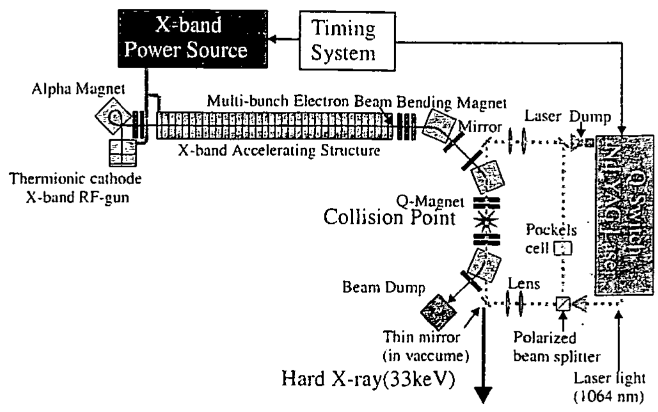

Fig. 3. Schematic illustration of the compact hard X-ray source based on a thermionic-cathode X-band RF gun, an X-band accelerating structure, a Q-switch Nd:YAG laser and a laser circulation system.

electron collision. After the collision, the electron beam is bent and decelerated by an X-band decelerating structure. The decelerated electron beam with an energy lower than 1 MeV is injected to a beam dump.

It is expected that beam loss at the beam-line is very small (less than 0.5%), because tailing of the bunch is suppressed at the beam-slit in the alpha-magnet. The radiation at the beam dump is dominant. We expect that radiation from the beam dump for a 1 MeV beam is less than 50 MeV and a heavy radiation shield is not needed. Details of the estimation for beam loss at the whole beamline in the final target system using PARMELA will be reported in another paper.

The laser system for collision is composed of a Q-switch Nd:YAG laser and a laser pulse circulating system to increase X-ray yield.

To demonstrate that the proposed X-ray sourse can be realized and will be useful in medicine, an X-band linac beamline for the proof-of-principle experiment shown in Fig. 3 is under construction.

In this paper, we present the design and numerical analysis of the X-ray source system to demonstrate hard X-ray generation and its applications.

2. Design and Numerical Analysis

2.1 *Choice of the laser systems and electron source*

First, we choose the laser system and electron source. To concentrate on the development of the accelerator, we choose a commercial and reliable laser for laser-electron collision.

X-ray yield, X-ray stability, and the size of the laser system are compared for the X-ray source with various lasers. Details of the calculation of X-ray yield are shown in §2.4. The thermionic cathode and photo-cathode RF gun can be chosen for electron source.

Calculated X-ray yields of various lasers are summarized in Table I.

The laser chosen is an ultra-short Ti:sapphire Tera watt (TW) laser. A single bunch, short pulse electron beam and an ultra-short laser pulse can generate short-pulsed X-rays with pulse lengths less than 10 ps (FWHM), but such a system requires subpicosecond timing control for X-ray stability, and the laser system is both expensive and not very stable.

Nd:Grass laser system can generate high intensity short pulse X-rays, but it is a huge system and the repetition rate of operation is very low.

A laser pulse stacking system is based on a Fabry-Perot cavity and continuous-wave (CW) mode-locked laser. The X-ray yield of this system that can enhance the laser power in the cavity depends on the enhancement factor N_{cav}. This system is not effective for a linac with a low repetition rate at $N_{cav} \sim 1000$, but is effective for small electron storage rings with high bunch populations above 100 MHz.

To realize such a compact system, we adopt the Q-switch Nd:YAG laser with a pulse energy 2 J/pulse, a repetition rate 10 pps, a pulse length 10 ns (FWHM), and a wavelength of 1064 nm. The commercial Q-switch laser system is compact, stable and reasonably priced. A multi-bunch electron beam

Table I. Summary of X-ray yields for various laser systems.

RF gun type	Electron beam	Laser	X-ray yield (photons)
Thermionic	20 pC/bunch	Q-switch Nd:YAG	1.7×10^7/pulse
-cathode	$\sim 10^4$ bunches/pulse	2 J/pulse, 10 ns, 10 pps	(1.7×10^8/s)
Thermionic	20 pC/bunch	Q-switch Nd:YAG	1.7×10^8/pulse
-cathode	$\sim 10^4$ bunches/pulse	+ Laser circulation system	(1.7×10^9/s)
Photo-cathode	500 pC/bunch	20TW Ti:Sapphire	1.6×10^7/pulse
		1 J/pulse, 50 fs, 10 pps	(1.6×10^8/s)
Photo-cathode	500 pC/bunch	Nd:Glass	2.1×10^8/pulse
		10 J/pulse, 10 ps, $\ll 1$ pps	
Photo-cathode	500 pC/bunch	15 nJ/bunch+pluse stacking	$6.2 \times N$/pulse
Multi-bunch	20 bunches/pulse	($15 \times N$) nJ/bunch, 7 ps	